

Observation of enhanced thermal noise due to multiple Andreev reflection in ballistic InGaAs-based superconducting weak links

著者	Akazaki Tatsushi, Nakano Hayato, Nitta Junsaku, Takayanagi Hideaki
journal or publication title	Applied Physics Letters
volume	86
number	13
page range	132505
year	2005
URL	http://hdl.handle.net/10097/51584

doi: 10.1063/1.1897851

Observation of enhanced thermal noise due to multiple Andreev reflection in ballistic InGaAs-based superconducting weak links

Tatsushi Akazaki,^{a)} Hayato Nakano, Junsaku Nitta, and Hideaki Takayanagi
*NTT Basic Research Laboratories, NTT Corporation, 3-1 Morinosato-Wakamiya, Atsugi-shi,
 Kanagawa 243-0198, Japan*

(Received 11 October 2004; accepted 21 February 2005; published online 25 March 2005)

We have experimentally obtained clear evidence of enhanced thermal noise in a ballistic superconductor-normal metal-superconductor junction with an InGaAs-based two-dimensional electron gas (2DEG). The thermal noise was estimated from a comparison of measured current-voltage characteristics with those obtained with an extended Ambegaokar and Halperin theory. As a consequence, we have observed enhanced thermal noise that is much larger than that expected with normal reservoirs. This enhanced thermal noise can be explained by a theory that considers both the ballistic transport of the 2DEG and the thermal fluctuation in the coherent multiple Andreev reflection regime. © 2005 American Institute of Physics. [DOI: 10.1063/1.1897851]

Current fluctuation is governed by both shot noise and Johnson–Nyquist noise (or thermal noise) after all extrinsic noise sources have been eliminated.¹ Shot noise is caused by the discreteness of the charge in an electrical current. When the current I is composed of independent shots, the shot noise takes the well-known Poissonian form $P=2qI$, where P is the noise power, and q is the effective charge transferred at each shot. The shot noise provides information on the correlation between electrons obtained by determining the effective charge, which is not contained in the conductance. During the last decade, a considerable amount of theoretical and experimental work has focused on the shot noise phenomena in mesoscopic superconducting junctions.² This is because the shot noise, namely the effective charge, is strongly affected by the peculiar nature of the charge transfer mechanisms arising from the presence of a Cooper pair condensate. In superconductor-normal metal (SN) junctions, the charge is transferred by the Andreev reflection (AR) process. An electron with energy E is retroreflected as a hole with energy $-E$ at the SN interface, and a Cooper pair enters the superconductor. Moreover, in SN-superconductor (SNS) junctions, the current proceeds through multiple AR (MAR).³ Here, quasiparticles travel back and forth between two superconductors, repeatedly removing Cooper pairs from one side and adding them to the other. When the coherence time is sufficiently long for the multiple reflections to be superposed coherently, this elementary process can carry a greater charge than an ordinary quasiparticle (electron or hole). As a consequence, MAR leads to an increase in the effective charge, and this means we can expect “giant” shot noise. This shot noise enhancement has been discussed theoretically and observed experimentally.² In contrast, little attention has been paid to thermal noise in the transport properties of mesoscopic SN (including SNS) junctions. This is because it has been believed that the thermal noise of a conductor does not provide any new information, since thermal noise is directly related to conductance G . Moreover, with a zero-bias voltage, the current is a nondissipative Josephson current. One would naively expect that the thermal noise at temperatures T smaller than the superconducting energy gap Δ_S ($k_B T \ll \Delta_S$) would be

negligible. However, with the superconducting quantum point contact (SQPC), the situation can be completely different due to the presence of the Andreev bound states in the N region between superconducting reservoirs.^{4,5} In such a mesoscopic SNS structure, MAR constructs discrete bound states. At a finite temperature, the upper level can be thermally populated giving rise to a reverse in the sign of the supercurrent. This switching between positive and negative current caused by thermal fluctuation leads to a huge increase in the thermal noise. Therefore, the thermal noise also provides information about the MAR process. In this letter, we report on the fabrication of a ballistic SNS junction with a two-dimensional electron gas (2DEG) in an InGaAs-based heterostructure.^{6–8} This ballistic SNS junction shows clear evidence of enhanced thermal noise. Thermal noise has been experimentally estimated from a fit of current-voltage (IV) characteristics, according to an extension of the Ambegaokar and Halperin theory.^{9,10} The experimentally obtained temperature dependence of thermal noise can be qualitatively explained by a theoretical description that considers both the ballistic transport of the 2DEG and the thermal fluctuation in the coherent MAR regime.

The InGaAs-based heterostructure was grown by metal-organic chemical vapor deposition on a semi-insulating (100) InP substrate. The sheet carrier density n_S and mobility μ of the 2DEG at ~ 0.35 K were found to be $2.07 \times 10^{12} \text{ cm}^{-2}$ and $129 \text{ 000 cm}^2/\text{V s}$ by Shubnikov-de Haas measurements. These values correspond to a mean-free path ℓ of $3.05 \mu\text{m}$. The Nb electrodes were coupled by the 2DEG in a 10 nm thick $\text{In}_{0.7}\text{Ga}_{0.3}\text{As}$ channel layer. The critical temperature T_C of the Nb electrodes was about 8.5 K . The coupling length L between the two Nb electrodes was about $0.17 \mu\text{m}$. The InGaAs channel width W was about $8.5 \mu\text{m}$.

Figure 1(a) shows the IV characteristics of the SNS junction at 0.36 K . A “superficial” critical current I_C^* of about $5 \mu\text{A}$ can be estimated from the current value at the corners of the IV characteristics (“real” critical current is discussed below). When a magnetic field is applied, the I_C^* follows a Fraunhofer pattern, as seen in Fig. 1(b). Here, the effective zero-magnetic field becomes $\sim 7 \text{ Gauss}$ due to the residual magnetic field. The periodicity becomes about one order of magnitude smaller than that corresponding to one flux quan-

^{a)}Electronic mail: akazaki@will.brl.ntt.co.jp

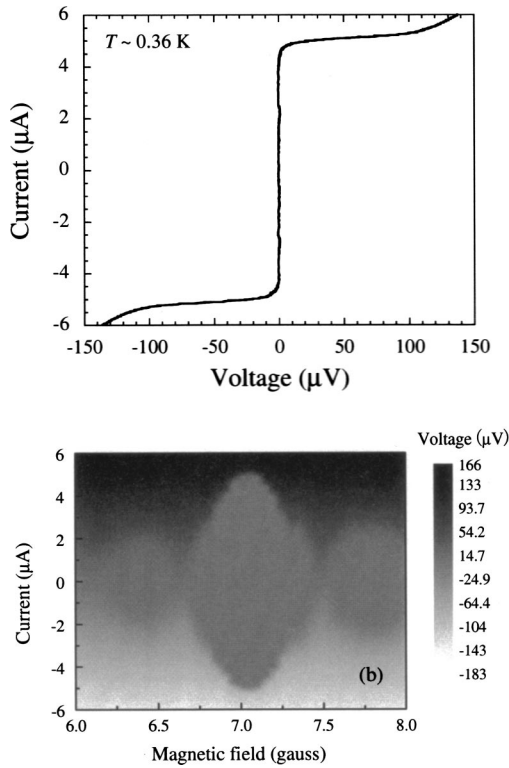


FIG. 1. (a) IV characteristics of the SNS junction at 0.36 K. (b) The output voltage of the SNS junction as a function of the input current and magnetic field at 0.36 K. The voltage is represented on a gray scale. The medium gray area, which represents a supercurrent, is identical to the Fraunhofer pattern.

tum inside the junction area. This discrepancy is caused by the flux enhancement resulting from the flux focusing within this geometry.¹¹ These features indicate that there is a Josephson current in this SNS junction. Figure 2 shows the differential resistance as a function of bias voltage V at 4 K. We obtained resistance minima within $|V|=2\Delta_S/e$ as well as dip structures near $|V|=2\Delta_S/ne$, with $n=1$ to 3 or 4. Here, we assumed the Nb superconducting energy gap Δ_S to be 1.2 meV, which is somewhat lower than the typical value of ~ 1.5 meV. A normal resistance R_N of $\sim 33 \Omega$ is obtained in the voltage region above $2\Delta_S$. These dip structures are the subharmonic energy-gap structures caused by the MAR. These results provide clear evidence that our SNS junction formed by 2DEG in an InGaAs-based heterostructure offers

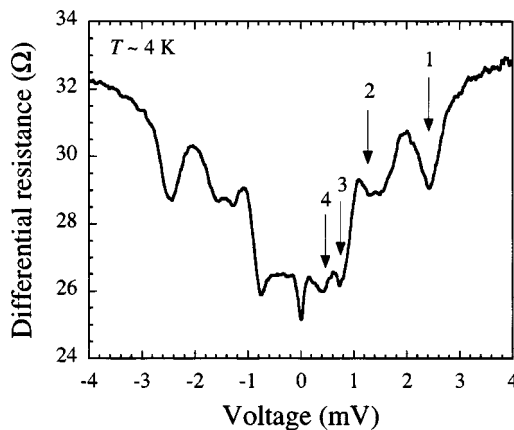


FIG. 2. The differential resistance of the SNS junction as a function of voltage at 4 K. The arrows indicate subharmonic energy-gap structures corresponding approximately to integer fractions of $2\Delta_S$.

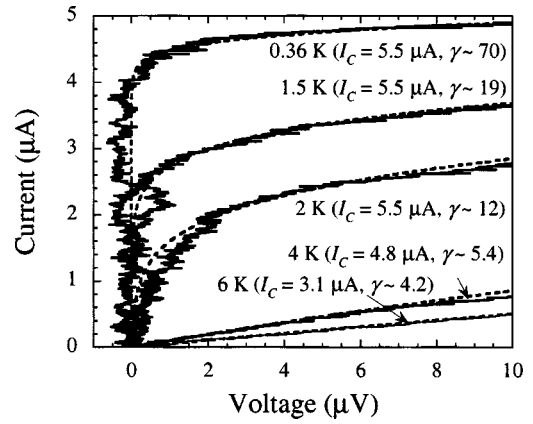


FIG. 3. The IV characteristics of the SNS junction measured at several temperatures. The solid and lines are experimental and calculated data for the low-voltage region below $\sim 10 \mu\text{V}$. The dimensionless parameter γ is determined so that it fits the measured IV curves.

ballistic transport in the 2DEG and sufficient transparency between Nb and the 2DEG.

Next, we estimated the thermal fluctuation of our ballistic SNS junction. We can quantitatively evaluate the effect of thermal fluctuation on the SNS junction from a fit of the IV characteristics, by using an extension of the Ambegaokar and Halperin theory including the additional term for phase-dependent dissipative current, namely the $\cos \phi$ term, proposed by Falco *et al.*¹⁰ Figure 3 shows the IV characteristics of the SNS junction measured at several temperatures. The dashed lines are the results of a parameter fit of the data to the theory in the low-voltage region below $\sim 10 \mu\text{V}$. Here, the dimensionless parameter $\gamma = \hbar I_C / ek_B T_{\text{noise}}$ is defined as a fitting parameter, where I_C is the real critical current and T_{noise} is the “effective” noise temperature. By using both an I_C of $5.5 \mu\text{A}$ and a γ of 70 at the lowest temperature of 0.36 K, we can obtain the best fit between the measured and calculated IV characteristics. In the low-temperature region, we can easily determine I_C since it almost the same as I_C^* . However, in the high-temperature region, it is hard to determine I_C due to the thermal noise. Therefore, the temperature dependence of I_C has been evaluated theoretically by fitting the I_C of $5.5 \mu\text{A}$ at 0.36 K to the calculated value. Since our SNS junction can be considered to be ballistic ($L \ll \ell$) and short [$L \ll \xi_0$, ξ_0 : Coherence length ($= \hbar v_F / \pi \Delta_S$), v_F : Fermi velocity in the normal region], the temperature dependence of I_C was calculated from the following expression for a ballistic and short SNS junction.^{12,13}

$$I(\phi, T) = \frac{e\Delta_S^2(T)}{2\hbar} \sin \phi \sum_{n=1}^M \frac{T_n}{E_n(\phi, T)} \tanh\left(\frac{E_n(\phi, T)}{2k_B T}\right), \quad (1a)$$

$$I_C(T) = \max I(\phi, T) \text{ at each } T. \quad (1b)$$

Here, the energy level of the Andreev bound state $E_n(\phi, T)$ is given by $E_n(\phi, T) = \Delta_S(T)[1 - T_n \sin(\phi/2)]^{1/2}$, where T_n is the transmission probability in the normal region and $\Delta_S(T)$ is the superconducting energy gap. For our SNS junction, we assume that $\Delta_S(0)$ is 1.2 meV and that the temperature dependence Δ_S is in accordance with the Bardeen–Cooper–Schrieffer theory. M is the number of transmission modes, which is given by $2W/\lambda_F$, [λ_F : Fermi wavelength of 2DEG]. For simplicity, we approximate that all transmission modes are equivalent. The T_n of ~ 0.4 is given from $T_n = R_{\text{sh}}/R_N$,

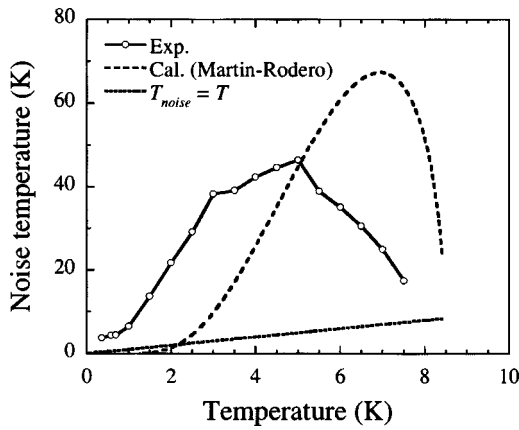


FIG. 4. The temperature dependence of the noise temperature of the SNS junction. The open circles with the solid line indicate the experimentally obtained noise temperature from the comparison with an extension of the Ambegaokar and Halperin theory. The dashed line represents the calculated temperature dependence of the noise temperature according to the Martín-Rodero theory. The dotted line represents the environment temperature T .

[R_{sh} Sharvin resistance of 2DEG, $R_{\text{sh}} = (h/2e^2)(\lambda_F/2W)$]. The calculated I_C from Eq. (1) at 0.36 K was about one order of magnitude larger than the estimated value of $5.5 \mu\text{A}$. The reason for this discrepancy is not yet clear. One possibility is that the effective number of transmission modes carrying the supercurrent is smaller than the above-estimated number of M . As shown in Fig. 3, we determined the fitting parameter γ using the evaluated I_C . As a consequence, we can evaluate the temperature dependence of T_{noise} from the evaluated I_C and γ . Figure 4 shows the temperature dependence of T_{noise} of the SNS junction. We found that T_{noise} is larger than the environment temperature T , represented by the dotted line in Fig. 4 as well as an exponential increase with increasing temperature in the sufficiently low-temperature regime where the decrease in Δ_S can be disregarded. The theory of thermal noise in SQPC can explain these results as follows.⁴ Martín-Rodero *et al.*⁴ have theoretically studied the frequency-dependent current fluctuations in SQPC within the dc transport regime. The zero-frequency thermal noise in SQPC is given by

$$P_{\text{SQPC}}(\phi, T) = \frac{2e^2 \pi \Delta_S^4(T) T_n^2 \sin^2 \phi}{h \eta E_n^2(\phi, T)} f(E_n(\phi, T)) \times [1 - f(E_n(\phi, T))]. \quad (2)$$

Here, $f(E)$ is the Fermi distribution function. η is the small energy relaxation rate that takes into account the damping of quasiparticle states due to inelastic processes inside electrodes. A typical estimation of η for a traditional superconductor is $\eta/\Delta_S \sim 10^{-2}$.⁴ Thermal noise power P_{SQPC} is di-

rectly related to both the noise temperature and the conductance by the fluctuation dissipation theorem,¹⁴ $P_{\text{SQPC}} = 4k_B T_{\text{noise}} G$. We use the estimated T_n of ~ 0.4 as well as $G = (2e^2/h) \times T_n$. The calculated temperature dependence of T_{noise} is shown by the dashed line in Fig. 4. The calculated curve shows the exponential increase with increases in temperature, which agrees qualitatively with the measured temperature dependence of T_{noise} . Moreover, the maximum value of $T_{\text{noise,cal}}$ is much larger than that of T . The above indicates that the experimental results are not explained by the thermal noise with normal reservoirs but by the enhanced thermal noise of the ballistic SNS junction. It should be noted that the experimental curve shifts toward a lower temperature than the calculated curve. The reason for this shift is not yet clear. One possibility is that the electron temperature in the 2DEG channel is higher than the reservoir temperature in the S .¹⁵ We must undertake further experimental work to explain the experimental results quantitatively. However, the experimentally obtained enhanced thermal noise can be qualitatively explained by the Martín-Rodero theory.

In conclusion, we have investigated the superconducting properties of a ballistic SNS junction with a 2DEG in an InGaAs-based heterostructure. We have observed the Josephson current as well as the subharmonic energy-gap structures caused by the MAR. Moreover, we experimentally estimated the thermal noise by comparing measured IV characteristics with those obtained with an extension of the Ambegaokar and Halperin theory. As a consequence, we have observed enhanced thermal noise. This enhanced thermal noise can be explained by a theory that considers both the ballistic transport of the 2DEG and the thermal fluctuation in the coherent MAR regime.

¹W. Schottky, Ann. Phys. **57**, 541 (1918).

²*Quantum Noise in Mesoscopic Physics*, edited by Y. V. Nazarov, NATO Science Series II/97 (Kluwer Academic Publishers, Dordrecht, 2003).

³M. Octavio, M. Tinkham, G. E. Blonder, and T. M. Klapwijk, Phys. Rev. B **27**, 6739 (1983).

⁴A. Martín-Rodero, A. Levy Yeyati, and F. J. García-Vidal, Phys. Rev. B **53**, R8891 (1996).

⁵D. Averin and H. T. Imam, Phys. Rev. Lett. **76**, 3814 (1996).

⁶J. Nitta, T. Akazaki, and H. Takayanagi, Phys. Rev. B **46**, 14286 (1992).

⁷H. Takayanagi, T. Akazaki, and J. Nitta, Phys. Rev. Lett. **75**, 3533 (1995).

⁸T. Akazaki, H. Takayanagi, J. Nitta, and T. Enoki, Appl. Phys. Lett. **68**, 418 (1996).

⁹V. Ambegaokar and B. I. Halperin, Phys. Rev. Lett. **22**, 1364 (1969).

¹⁰C. M. Falco, W. H. Parker, and S. E. Trullinger, Phys. Rev. Lett. **31**, 933 (1973).

¹¹J. Gu, W. Cha, K. Gamo, and S. Namba, J. Appl. Phys. **50**, 6437 (1979).

¹²C. W. J. Beenakker, Phys. Rev. Lett. **67**, 3836 (1991).

¹³A. V. Galaktionov and A. D. Zaikin, Phys. Rev. B **65**, 184507 (2002).

¹⁴H. B. Callen and T. W. Welton, Phys. Rev. **83**, 34 (1951).

¹⁵T. Hoss, C. Strunk, T. Nussbaumer, R. Huber, U. Staufner, and C. Schönberger, Phys. Rev. B **62**, 4079 (2000).